



Biochar Derived from Peanut Husks As An Adsorbent to Ammonium Ions Remediation from Aqueous Solutions

Ahmed F. M. Ali,¹ Abdelaal S. A. Ahmed,^{1*} Ahmed A. Gahlan^{1*}, Abdel-Aziz Y. El-Sayed¹



¹Chemistry department, Faculty of science, Al-Azhar university, Assiut 71524, Egypt

Abstract

Water pollution by ammonium ions is considered a critical environmental issue that arises from various fast developments in industrial, human, and agricultural activities. In this study, peanut husk powder (PH), PH modified with mixture NaOH and KMnO_4 (mPH), and its derived biochar (BPH) were prepared and characterized by Fourier transform infrared spectroscopy (FTIR), scanning electron microscope (SEM), and Brunauer-Emmett-Teller (BET) techniques. The obtained adsorbent materials were utilized for the remediation of ammonium ions from aqueous solution via batch approach. The effect of both pH, contact time, adsorbent doses, and initial ammonium concentration on the overall adsorption performance was systematically investigated. The maximum removal percentage of $\text{NH}_4(\text{I})$ was found to be 68, 97, and 78% for PH, mPH, and BPH, respectively. Furthermore, the adsorption kinetics, and isotherms for the adsorption of $\text{NH}_4(\text{I})$ onto all prepared three adsorbents were studied to show the behaviour of the adsorption process. The kinetic study displayed that the adsorption of $\text{NH}_4(\text{I})$ ions onto all adsorbent materials was fitted with the pseudo-second-order model. The adsorption isotherm showed that the adsorption of $\text{NH}_4(\text{I})$ ions was obeyed with the Langmuir model, which confirmed the formation of monolayer $\text{NH}_4(\text{I})$ ions onto the surfaces of the adsorbent materials. For the real applications, the mPH material was utilized for the removal of $\text{NH}_4(\text{I})$ ions from groundwater, wastewater, and a spiked Nile River sample, and the obtained data displayed a high ability of mPH toward $\text{NH}_4(\text{I})$ ions in all investigated samples which are important for large scale applications. In addition, all prepared adsorbent materials displayed high reusability without remarkably decreasing adsorption capacity. Thus, our work proved the promising ability of high peanut husk and its derivatives to be utilized as an adsorbent for the remediation of $\text{NH}_4(\text{I})$ ions from aqueous solutions.

Keywords: Wastewater treatment; inorganic pollutants; ammonium ions; low-cost adsorbents; adsorption isotherm

1. Introduction

Since water is used extensively in all facets of our lives, protecting our water supplies, and even treating wastewater is considered an urgent task for securing water suppliers for the coming generations. According to environmentalists, wastewater contains a range of pollutants, such as heavy metals, ammonia, and toxic organic non-degradable chemicals. Thus, releasing it into the environment without treatment is a bad idea that poses major challenges and puts the environment in danger as it is responsible for about 14,000 deaths daily, of which ammonium contaminants are the large contributors.[1] Despite its negative consequences, ammonia is a widespread raw material used in the production of animal feed, fertilizers, and various appliances, including those

that produce paper, rubber, textiles, plastics, and explosives.[2] Elevated levels of ammonia were mostly seen in groundwater, with a considerable human contribution near the mining and smelting of ammonia-containing ores.[3] Ammonia is the primary byproduct of protein catabolism and is expelled as ionized ammonia $\text{NH}_4(\text{I})$ and unionized ammonia (NH_3). Unionized ammonia is a critical indicator of water quality that is detrimental to aquatic life, even though ammonium ions are safe to eat in little doses. [4] The interchangeability of ammonium and unionized ammonia is possible based on the temperature and pH of both natural and urban waters. Unionized ammonia is significantly more toxic than ammonium because of its neutrality. However, ammonium is found in far higher levels

*Corresponding author e-mail: abdelaalsayid@gmail.com; (A.S.A. Ahmed).

EJCHEM use only: Received date 22 February 2024; revised date 08 May 2024; accepted date 03 June 2024

DOI: 10.21608/ejchem.2024.271974.9374

©2024 National Information and Documentation Center (NIDOC)

than ammonia because natural waters frequently have a pH that is circum-neutral. Drinking water with a high $\text{NH}_4(\text{I})$ level over an extended period will seriously endanger people's health. This is mainly because an excess of $\text{NH}_4(\text{I})$ can throw off the body's acid-base equilibrium. When ammonia is consumed at a daily dose exceeding 100 mg/kg of body weight (33.7 mg of ammonium ion per kg of body weight), it can disrupt the body's ability to metabolize glucose and reduce tissue sensitivity to insulin. [5] Furthermore, ammonia is responsible for headaches, nausea, diarrhea, and sleeplessness. It is known to be a potent cell toxin that targets the heart tissues and can harm fish gills at concentrations as low as 0.25 mg/L. [6]

Ammonia may enter the aquatic environment through indirect pathways including nitrogen fixation, air deposition, and runoff from agricultural areas, as well as direct pathways like animal waste emissions and municipal effluent discharges. [7] The release of wastewater leads to the stimulation of eutrophication, soil acidity, vegetation fertilization, corrosion and fouling, and changes in ecosystems. In addition, this component can be converted to nitrate in aerobic conditions, which eventually leaches into water resources, especially surface water and groundwater resources. [8,9] Also, concentrated ammoniacal nitrogen can be released into surrounding surface water bodies and groundwater sources by the seepage of leachate from poorly managed or unlined landfill sites. This can promote the growth of algae and reduce the amount of dissolved oxygen (DO) in water bodies. [10] Eutrophication typically leads to a decrease in DO (hypoxia and anoxia), the loss of fish and other aquatic life, the degradation of water quality, harmful algal blooms, as well as decreases in the recreational value of the water. [11] Therefore, controlling N from the main sources is extremely important. Recently a lot of chemical, physical, and biological techniques were developed for the remediation of ammonia from wastewater. Unfortunately, the biological treatment processes (e.g. nitrification and denitrification) and physical treatments (e.g. electro dialysis and reverse osmosis) both are high-cost procedures. Chemical processes such as precipitation, reduction, and adsorption are considered the most widely used methods due to their simplicity, safe time, and relatively low cost. [12]

Adsorption is an important technique for the remediation of ammonia from their aqueous solutions. The adsorbent materials play a critical role in the overall cost and adsorption performance. Thus, it's important to choose an effective, plentiful, inexpensive, eco-friendly adsorbent materials. [13] Till now, various adsorbent materials including carbons, [14] metal oxides, [15] and so on have been utilized as effective adsorbent materials for the remediation of ammonia from water. Recently, agricultural waste materials have been utilized as effective adsorbents due to their natural availability at about no cost. In addition, the management and re-use of waste materials is considered an urgent need for our plant. [16] Thus, using it as an adsorbent is an attractive option from both economic and environmental points of view. [17,18] Typically, agricultural waste materials containing an average content of 40-50% cellulose, 20-30% hemicellulose, 20 -25% lignin, and 1-2% ash, thus considered abundant sources of cellulosic material and an appealing source for carbon synthesis. [17] These materials contain various functional groups such as hydroxyl, aldehyde, carbonyl, carboxyl, phenolic, and/or ether groups which can interact with a range of different contaminants in wastewater. [19] However, the low adsorption capacity of agriculture wastes is the main challenge that needs to be addressed. Great efforts have been devoted to addressing this point. These processes mostly include the use of bases, organic acids, oxidizing agents, organic compounds, and mineral acids treatments. Various chemical reagents such as $\text{Ca}(\text{OH})_2$, Na_2CO_3 , NaOH , HNO_3 , HCl , H_2SO_4 , H_3PO_4 and KMnO_4 have been used to improve the adsorption capability of adsorbents. [20] Usually diluted NaOH solution is used to boost the sorption capacity as well as to enhance the penetration of modifying agents. [21] On the other hand, KMnO_4 is used as a reducing agent toward the organic functional groups, which increases the amount of oxygen-containing groups on the surface and thus improves the ability of the treated biomass to adsorb substances. Conversely, the biomass surface produces new ecological and biological MnO_2 ($\delta\text{-MnO}_2$) that is capable of absorbing cations from wastewater. [22] The other important way agriculture wastes is the conversion to high porosity, hydroxy-rich, and high-carbon solid biochar via pyrolyzed at a suitable temperature in

anoxic or oxygen-limited environments for utilizing as adsorbent.[23,24] Agricultural wastes, such as straw, fruit shells, food scraps, and plant stalks are typically favored as biochar feedstock due to their accessibility, affordability, lack of toxicity, and ability to mitigate waste issues. Biochar is considered a promising adsorbent material due to its high surface area, hydrophobicity, microporosity, and the presence of various functional groups (C–O, –OH, –COOH) Thus, it has proven possible to effectively extract both organic and inorganic materials from aqueous solutions using biochar. [13,25]

Peanut husk (PH) are a famous agricultural waste in Egypt and many countries and are produced in large quantities. PH is often utilized as an animal feed, substrate, fertilizer, or fuel. In addition, utilized as an adsorbent to remove various organic pollutants, heavy metals, and from their aqueous solutions.[26] However, according to our knowledge there is no literature about utilizing PH or its derivatives for the remediation of ammonia from aqueous systems. Thus, in our study we utilized three PH based adsorbents for remediation of ammonia from wastewater via batch adsorption approach. These adsorbents are PH powder, PH modified with KMnO_4 and NaOH , and PH-derived biochar. The effect of pH, contact duration, dose of the adsorbent, and initial ammonia concentration on the overall adsorption will systematically be investigated. The adsorption kinetics and isotherm will also be examined to show the behavior of the adsorption process. The reliability of the adsorbent materials for many times will be included. Furthermore, the behavior of our adsorbent materials toward the real samples will be investigated.

2. Materials and methods

2.1 Chemicals and reagents

All chemicals were analytical grade: sodium hydroxide (NaOH , $\geq 98\%$, pellets anhydrous), hydrochloric acid (HCl , 37%), ethanol absolute alcohol ($\text{C}_2\text{H}_5\text{OH}$, $\geq 95\%$), ammonium chloride (extra pure 99.5%), nitric acid ($\text{HNO}_3 \geq 65\%$), phenol, potassium permanganate ($\text{KMnO}_4 \geq 99\%$), sodium nitroprusside ($\text{Na}_2[\text{Fe}(\text{CN})_5] \cdot \text{NO} \cdot 2\text{H}_2\text{O}$, $> 99\%$), trisodium citrate ($\text{C}_6\text{H}_5\text{Na}_3\text{O}_7 \cdot 2\text{H}_2\text{O} > 99\%$), and sodium hypochlorite (6–14%) were purchased from Merck, Darmstadt, Germany. All reagents were of analytical purity and were used without further purification. All preparations in our study were performed with distilled water obtained from an

ultra-pure purifier (Ulupure, resistivity $\geq 18.2 \text{ M}\Omega$).

2.2 Preparation of adsorbent derived from PH.

Our work includes the preparation of three adsorbent materials: PH powder, m-PH, and BPH as described in the following scheme 1. The PH waste was collected from agricultural lands located in Awlad Salem Bahri village, Dar-Elsalam city, Sohag, Egypt.

2.2.1 Prepare pure PH

The gathered PH waste was washed thoroughly with tap water to remove the dust, then washed once with distilled water and finally dried at 100°C for 12h in an oven. The dried PH material was finely powdered and sieved to a $63 \mu\text{m}$ particle size. After that, the pulverized PH was packed into a pristine plastic polypropylene air tightly bottle, and the resulting powder was called PH.

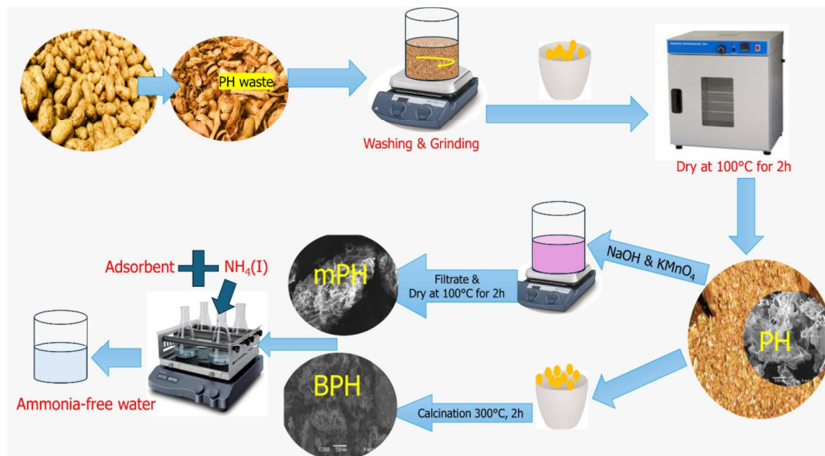
2.2.2 Prepared modified PH (m-PH)

For the chemical-modified PH, a certain weight of dry PH was suspended for 30 min in a mixture of 0.01M NaOH + traces of KMnO_4 until the solution became slightly pink with a solid-liquid ratio of 0.005g/0.25mL at temperature 25°C . After that, the biomass was washed with distilled water several times until $\text{pH} \approx 7$. After decantation the filtrate was discharged and the biomass (mPH) was dried in an oven at 100°C for 2h, ground well with a mortar and then packed in clean plastic polypropylene air tightly bottles, the obtained powder was designated as mPH.

2.2.3 Prepared biochar-derived PH (BPH)

For biochar-derived PH, a certain weight of PH is placed into a ceramic vessel that is closed with their respective caps. This vessel was custom-made not to allow oxygen to enter the vessel at high temperatures. The vessel was placed in a gradient temperature furnace at a temperature of 300°C for 2h. The mass of material after the pyrolysis process, grounded well with a mortar and was packed in clean plastic polypropylene air tightly bottles, the obtained black material was designated as BPH.

We should highlight that the cost of our prepared adsorbent materials for the possibility of was not much as we use a PH waste material without money, and in all next step the cost was limited as we use only very dilute NaOH , traces KMnO_4 , and the dry and calcination process. Thus, we could say that these prepared materials are cost-effective. The whole process for preparing the PH-derived adsorbents is shown in scheme 1.



Scheme 1: The procedure for preparing PH-derived adsorbents.

2.3 Characterization and measurements

To prepare the samples, the following equipment was used: an orbital shaker (BTC Model BT4010, Egypt); a pH meter (Adwa Model AD110, Romania); a drying oven (bender, Germany); a spectrophotometer instrument (model: CECIL3021, Cambridge, England); shaking standard testing sieves (model: FTL0200 “IRIS”, Filtra, Spain); a muffle furnace (LH 60/12, Nabertherm GmbH, Germany); grinding (food processor); and a Sartorius balance (model ED224S and Germany). The functional groups included in the adsorbents were identified using FTIR (Nicolet 6700, Thermo Fisher, USA). For measuring mean pore diameter, total pore volume, and specific surface area, use BET (BEL SORP MAX, Japan). The scanning electron microscopy (SEM; model JEOL JSM-5500 LV, Japan), ICP-OES (Inductively Coupled Plasma-Optical Emission Spectroscopy model Quantima-GBC, made in Australia), IC (Ion Chromatography model S 153-A Sykam GmbH, Germany), Conductivity/TDS Meter (model 4510 Jenway, made in England), the grinding mortar, the glassware flasks, the glassware (beakers, cylinders, pipettes, clear glass bottles, funnels, and ceramic vessel with cap), the polypropylene bottles, and the filter paper whatman were utilized in the field tests.

2.4 Adsorption ammonium ions

The adsorption processes of ammonium ions were performed with a lab shaker. Each experiment was run at least three times, and mean values were taken. The effects of solution pH, contact time, initial ammonium concentration, and adsorbent dosage on the adsorption efficiency of our prepared materials were investigated by batch adsorption technique using a lab shaker with an agitation speed of 130 rpm, and at $25 \pm 1^\circ\text{C}$. In each experiment, 0.1g of adsorbent material was mixed with 50 mL of ammonium solution at an initial concentration of 10 ppm. The solution pH was adjusted by 0.01M HNO_3 and 0.01M NaOH solutions. The mixture was shaken for an appropriate time followed by filtration and the remaining concentration of ammonia was analyzed by the phenolate method using a UV-visible spectrophotometer. The removal percent (R%) of $\text{NH}_4(\text{I})$ was determined by Eq. 1, and the adsorption capacity (q_e ; mg/g) was measured by Eq. 2.

$$R (\%) = \frac{C_0 - C_e}{C_0} \times 100 \quad (\text{Eq. 1})$$

$$q_e = \frac{(C_0 - C_e)}{M} V \quad (\text{Eq. 2})$$

Where C_0 and C_e are the initial and final $\text{NH}_4(\text{I})$ concentrations (mg/L), respectively. V is the solution volume (L), and M is the adsorbent mass (g).

3. Results and Discussion

3.1 Characterization of the adsorbent

N_2 was used as the adsorbate and the samples of adsorbent material were subjected to Brunauer-

Emmett-Teller (BET) surface area measurements at 77K (-196°C). **Table 1** shows that the change has enhanced the pore volume and specific surface area. Additionally, heat action caused a rise in BPH's pore capacity and specific surface area. When raw

materials were pyrolyzed at a high temperature, several gases, including CO₂, were released, which increased the pore width of BPH. The pore's diameter decreased because of the modification's ability to embed several functional groups in the PH pore.

Table 1: BET specific surface area, pore volume and pore diameter of the adsorbent materials.

Biosorbent	BET (m ² /g)	Pore volume (cm ³ /g)	Mean pore diameter (nm)
PH	2.35	0.13	20.94
mPH	7.41	5.25	2.83
BPH	9.83	6.22	25.32

FT-IR spectral analysis is important in identifying the different functional groups on the biosorbent surface that are responsible for the adsorption of NH₄⁺ ions. As in **Figure 1**, the PH showed the presence of O–H, N–H, C–H, C=O, C=C, C–N, C–O and C–H vibrations on the surface, thereby providing sufficient surface functionality for pollutant interaction. The broad band of O–H and N–H groups at 3409 cm⁻¹. The presence of peak at 2122 cm⁻¹ might be due to the presence of C≡C bonds. The bands centered at 1736 cm⁻¹ and 1642 cm⁻¹ are due to the stretching vibrations of C=O groups. The C=C stretching vibrations of the aromatic ring of lignin at 1512 cm⁻¹. In addition, the presence of aromatic methyl (–CH₃) group vibrations at 1452 cm⁻¹ was compatible with the presence of the aliphatic part of

lignin. The peak at 1379 cm⁻¹ represents aliphatic C–H stretching in methyl and phenol alcohols. The peaks between 1321cm⁻¹ and 1034 cm⁻¹ can be attributed to C–O stretching vibrations of carboxylic groups. The bands that appeared below 1034 cm⁻¹ cannot be recognized easily because it is the fingerprint region and contain complex vibrating interactions. Modification leads to shifts in some groups, and the band 1034 cm⁻¹ disappeared. Pyrolysis leads to shifts in some groups, the appearance of peaks 2852 and 1583 cm⁻¹ can be attributed to dehydration, dehydrogenation, and deoxygenation reactions at elevated temperatures. In summary, FT-IR of PH demonstrated the existence of certain functional groups that are active and cause ammonium ions to be adsorbed.[27]

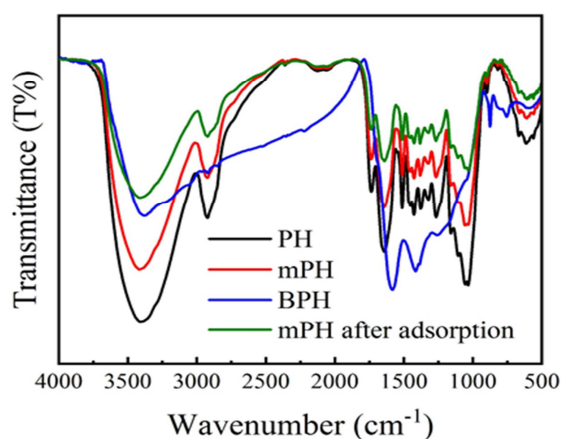


Figure 1: FT-IR spectra of PH, mPH, BPH adsorbents and mPH after adsorption.

To investigate the morphology of the materials, SEM was applied. From **Figure 2**, the surface morphology of the samples PH and mPH are clearly different, and the surface of mPH is porous. The morphology of PH and mPH samples after adsorption displayed a different morphology as the surface is transformed to be more compact,

smoother, and less open pores are seen due to the bounding of the ammonium ions on the mPH surface. The SEM in **Figure 2c** revealed that the BPH had a rough, and irregularly sized, and shaped highly porous surface with multiple voids and micropores, providing sufficient space for the adsorption process.

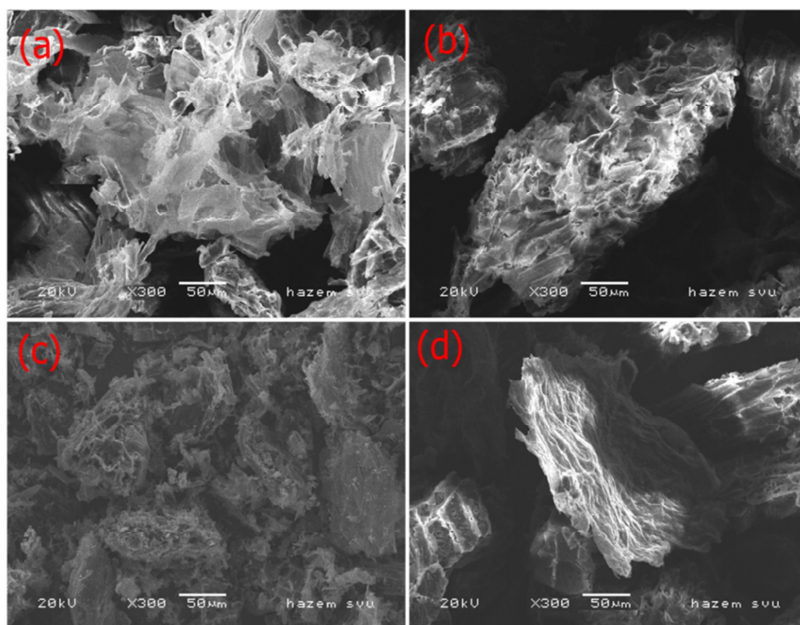


Figure 2: SEM images of (a) PH, and (b) mPH before adsorption. SEM images of (c) BPH, and (d) mPH after adsorption.

3.2 Adsorption study

The effect of pH on the adsorption of $\text{NH}_4(\text{I})$ for PH was shown in **Figure 3a**. Results generally showed that the maximum ammonium ion adsorption behavior occurred at high pH values. The other parameters were kept constant. The initial pH values of the solutions were detected by adding 0.01M HNO_3 and 0.01M NaOH solutions to reach the desired value. The removal percentage of PH for $\text{NH}_4(\text{I})$ increased with increasing $\text{pH} \approx 7$. The increase in removal percentage with increasing pH could be demonstrated due to the degree of ionization and the charge on the adsorbent surface. At low pH, the highly movable H^+ would interact with the ammonium ions at the active sites. Thus, the binding sites become protonated, resulting in a decrease in the

ammonium ions sorption on the adsorbent surface. At high pH, the H^+ concentration and the solubility of ammonium ions were decreased, which enhanced the sorption of ammonium ions on the adsorbent surface. Studies on higher pH (alkaline) values were not preferred where ammonium ions are converted into ammonia through volatilization and the ammonia molecules cannot exchange back into the adsorbent and thus are stripped of air, causing a decrease in ammonium ions removal. Therefore, all steps of the adsorption process were carried out with a pH of 7. The effect of adsorbent dosage on the removal percentage of $\text{NH}_4(\text{I})$ ions from synthetic wastewater is shown in **Figure 3b**, where the optimum dose for $\text{NH}_4(\text{I})$ ions was 0.15g. It was observed that as the weight of biomass increased, a gradual increase in the removal percentage was obtained for $\text{NH}_4(\text{I})$ ions.

This referred to the increasing sportive surface area, and the active binding sites were more available on the adsorbent surface with increasing of the adsorbent dose. Further, any increase in the adsorbent dosage will not have any major changes.[28] The effect of different adsorption times on the removal percentage of $\text{NH}_4(\text{I})$ using PH were shown in **Figure 3c**, where the optimum contact time for the $\text{NH}_4(\text{I})$ ions was 100 min. The other adsorption conditions were kept

constant during the study. The removal percentage gradually increased, then slowed down until reaching the equilibrium state with time. This was due to the reaction of the functional groups of the PH with the $\text{NH}_4(\text{I})$ ions and thus the adsorption sites gradually became occupied. The removal of $\text{NH}_4(\text{I})$ ions reached its maximum limit when the adsorption sites and functional groups of PH were close to saturation.

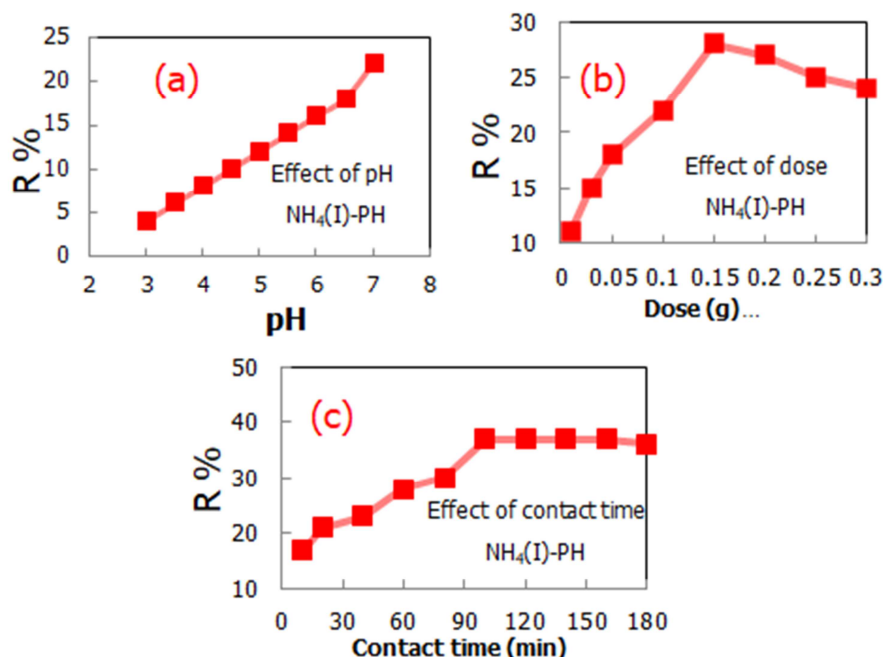


Figure 3: Effect of (a) solution pH (pH 3-7; dose 0.1g, 60 min), (b) adsorbent dosage (dose =0.01-0.3g; pH= 7; contact time 60 min) (c) contact time (pH 7; dose 0.15g; contact time = 10-180 min) on the removal of ammonium ions from aqueous solution by PH.

A comparative sorption study was accomplished with non-modified, modified, and biochar peanut husk to deduce the sorption efficiency of the sorbents. The effect of modification and pyrolysis of PH on the adsorption of $\text{NH}_4(\text{I})$ is shown in **Figure 4**, where the results of $\text{NH}_4(\text{I})$ adsorption tests with PH before, after modification, and after pyrolysis. The $\text{NH}_4(\text{I})$ ions concentrations were explained in the range of 5 to 25 mg/L with a fixed optimum

parameter of pH, contact time, and dose as illustrated before. The removal capacity of $\text{NH}_4(\text{I})$ ions were decreased by increasing concentrations from 68 to 17% for PH, from 97 to 26% for mPH and 78 to 33% for BPH. Thus, the removal efficiency was decreased by increasing $\text{NH}_4(\text{I})$ ions concentrations in the solutions. By increasing the $\text{NH}_4(\text{I})$ ion concentration, the number of sorption sites in a certain mass of an adsorbent substance became saturated.

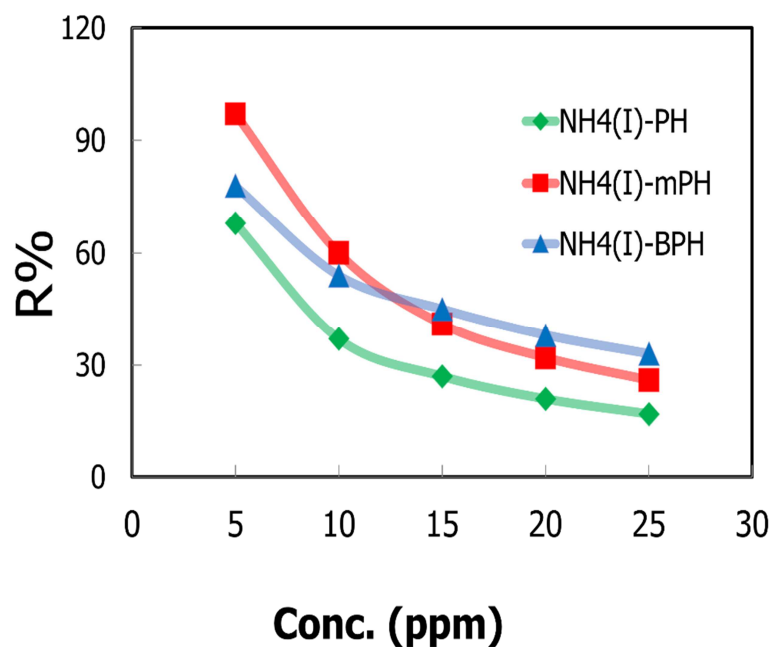


Figure 4: Effect of conc. for PH, mPH and BPH.

3.3 Adsorption isotherms

Ammonium ions sorption data were correlated with the Langmuir (Eq. 3) and Freundlich (Eq. 4) models. [27]

$$\frac{C_e}{q_e} = \frac{1}{(q_{\max} * b)} + \frac{1}{q_{\max} * C_e} \quad (\text{Eq. 3})$$

$$\text{Ln}q_e = \text{Ln}K_f + \left(\frac{1}{n_f}\right) \text{Ln}C_e \quad (\text{Eq. 4})$$

Where C_e is the $\text{NH}_4(\text{I})$ ions concentration at equilibrium (mg/L), q_e the $\text{NH}_4(\text{I})$ ions amount sorbed at equilibrium (mg/g), q_{\max} the maximum sorption

capacity, b is the Langmuir constant, K_f and n_f are the Freundlich constants.

Langmuir and Freundlich isotherm models of the biosorption of $\text{NH}_4(\text{I})$ onto PH, mPH and BPH at 25 ± 1 °C were reported in Table 2. The correlation coefficient values (R^2) illustrated that the Langmuir isotherm model was best prepared for the biosorption of $\text{NH}_4(\text{I})$ ions on PH and mPH and that the Freundlich isotherm model was best prepared for the adsorption of $\text{NH}_4(\text{I})$ ions on BPH as in Figure 5(a, b). [30]

Table 2: The parameters estimated from adsorption isotherm models for the Ammonium ions adsorption on PH, mPH and BPH.

Adsorbent	Langmuir			Freundlich		
	q_{\max} mg/g	B L/mg	R2	K_f (mg/g).(L/mg) ^{1/n}	n_f	R2
PH	1.454	1.260	0.998	1.085	11.876	0.9708
mPH	2.158	4.061	0.999	1.82	17.153	0.9871
BPH	3.079	0.395	0.985	1.220	3.516	0.9934

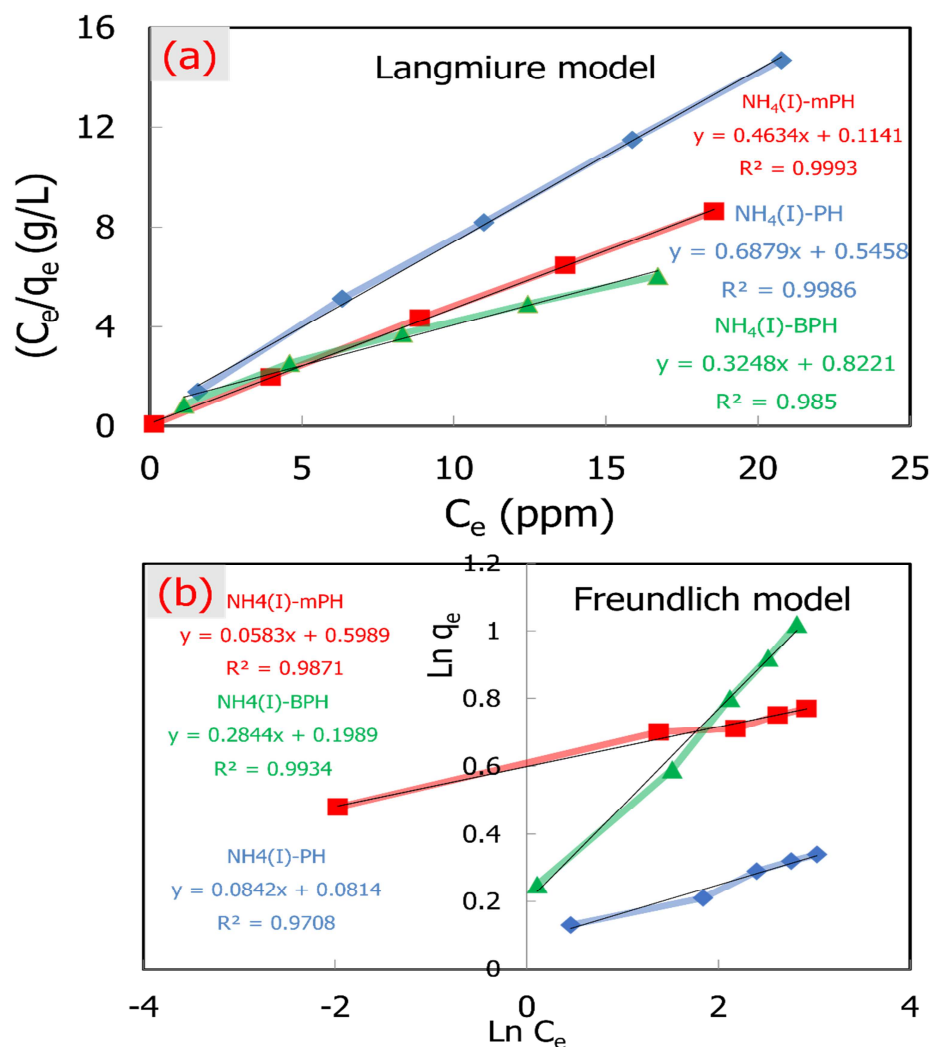


Figure 5: Langmuir, and Freundlich adsorption isotherm models for adsorption ammonium ions onto PH, mPH, and BPH.

3.4 Adsorption kinetics

This work examined and described the adsorption kinetics of ammonium ions using the pseudo-first order, pseudo-second order, and intra-particle diffusion rate kinetic models. [29,30] A pseudo-second-order equation based on the adsorption equilibrium capacity could be expressed in **Eq. 6**, the pseudo-first equation representing the adsorption of a solute from a liquid solution was shown in **Eq. 5**, and **Eq. 7** represented the intra-particle diffusion rate that increased with an increase in initial concentrations.

$$\ln(q_e - q_t) = \ln q_e - K_1 * t \quad (\text{Eq. 5})$$

$$\frac{t}{q_t} = \frac{1}{(k_2 * q_e^2)} + \frac{t}{q_e} \quad (\text{Eq. 6})$$

$$q_t = k_p * t^{\frac{1}{2}} + C \quad (\text{Eq. 7})$$

where q_e is the adsorbed ammonium ion mass at equilibrium (mg/g), q_t is the adsorbed ammonium ions mass at time t (mg/g), K_1 is the pseudo-first order reaction rate constant (l/min), and K_2 is a constant that represents the pseudo second-order reaction rate equilibrium (g/mg min), K_p is the rate constant of intra-particle diffusion (mg/g.min^{1/2}) and C (mg/g) is the intercept, which is identified with the thickness of the boundary layer, and $t^{1/2}$ (min) represents the square root of time.

Figures 6 and Figure 7 (a,b) display the plots of the three kinetic models. Table 3 enumerates the relevant kinetic parameters. q_e values were closer to experimental results, and the pseudo second order

equation could adequately reflect the predicted models for ammonium ions and the associated statistical parameters that relied on linear regression data (R^2).

Table 3: Parameters of the pseudo-first, pseudo-second-order kinetic, and intra-particle diffusion models of the adsorption of ammonium ions on PH, mPH and BPH.

Kinetic model	Parameter	Adsorbents		
		PH	mPH	BPH
Pseudo-first order	q_e (mg/g)	1.23	2.04	1.80
	q_t (mg/g)	1.04	0.70	0.81
	K_1 (min^{-1})	0.028	0.013	0.01
	R^2	0.825	0.855	0.898
Pseudo-second order	q_e (mg/g)	1.23	2.04	1.80
	q_t (mg/g)	1.40	2.05	1.76
	K_2 (g/mg. min)	0.032	0.006	0.05
	R^2	0.987	0.996	0.989
Intra-particle diffusion	K_{id} ($\text{mg/g. min}^{0.5}$)	0.071	0.06	0.07
	$q_{e,exp}$ (mg/g)	1.23	2.04	1.80
	$q_{e,cal}$ (mg/g)	0.38	1.21	0.83
	R^2	0.924	0.859	0.811

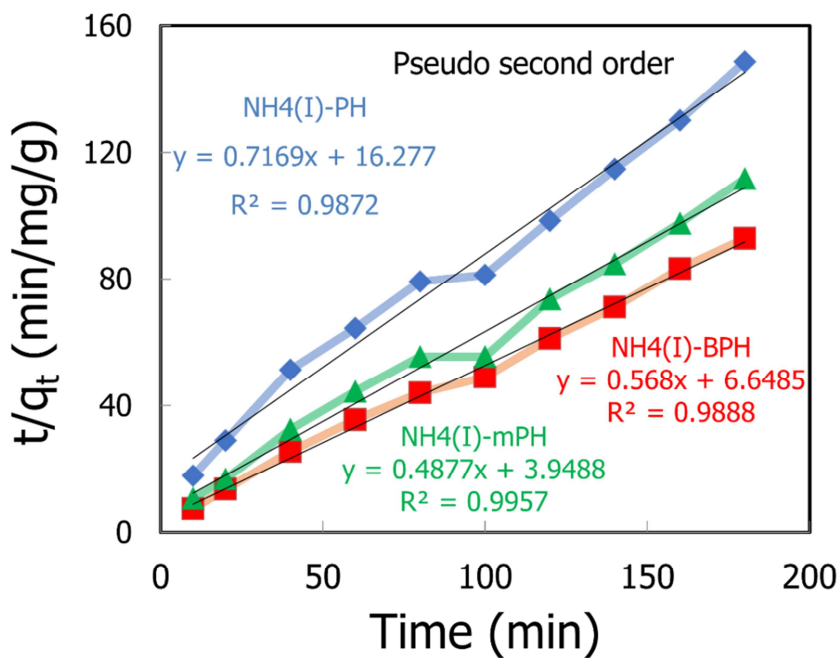


Figure 6: Pseudo second order model for PH, mPH and BPH.

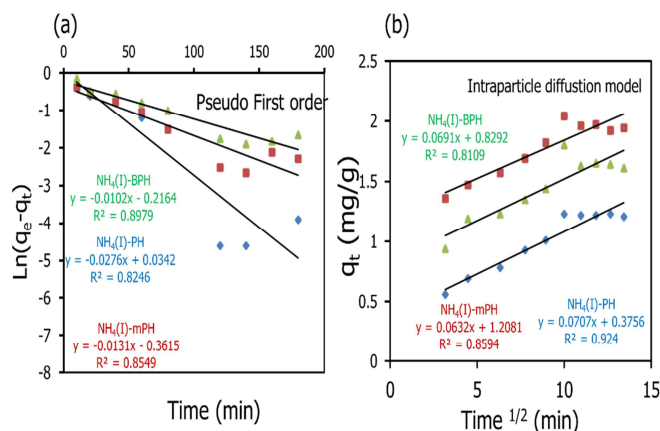


Figure 7: (a) Pseudo first order, and (b) Intraparticle diffusion models for PH, mPH and BPH.

3.4.1 Regeneration of the adsorbent materials

For effective adsorption-based pollutant sequestration, the sorbent must be recyclable without experiencing a significant decline in its adsorption capability.[33] The ability to utilize adsorbent materials in several ways is crucial for lowering the overall cost of the treatment procedure. Here, the reusability of the PH, mPH and BPH adsorbent materials was investigated by monitoring their adsorption toward $\text{NH}_4(\text{I})$ under ideal conditions for five cycles. Adsorption was conducted at solid/liquid ratio of 0.15g/50ml at room temperature (25°C) at contact time 100 min with 5ppm ammonium concentration. Then, the regeneration studies were

conducted by washing the $\text{NH}_4(\text{I})$ -adsorbed onto PH, mPH and BPH materials with 1% NaCl for 30 min at room temperature. After that, the regenerated PH, mPH and BPH were reused for $\text{NH}_4(\text{I})$ adsorption, and five cycles of regeneration and adsorption were carried out in succession. Figure 8 displays that both PH, mPH and BPH materials depict good recyclability after five cycles of desorption-adsorption. As shown in Figure 8, the removal percentage of $\text{NH}_4(\text{I})$ decreased by 19.12%, 22.68 and 21.79% onto PH, mPH, and BPH, respectively. Thus, the PH, mPH and BPH materials are highly reusable for the removal of $\text{NH}_4(\text{I})$ from wastewater.

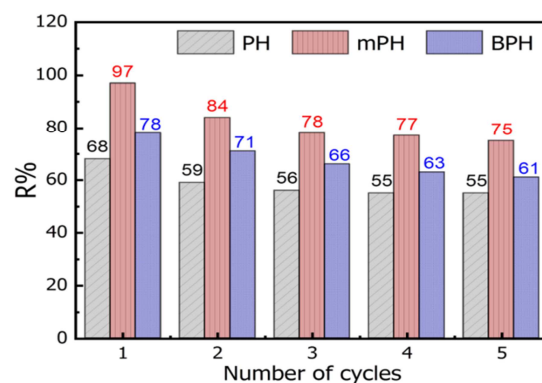


Figure 8: Regeneration of the PH, mPH and BPH up to five successive desorption-adsorption cycles

4. Application of mPH for real samples

The removal capacity of ammonium ions by the mPH for real samples from ground water, wastewater after the tertiary treatment process, and a spiked Nile

River sample are shown in **Table 4** with an estimation of total dissolved salts (TDS) as well as the pH.

Table 4: Application of NH₄ (I) ions removal by mPH for real samples

Total dissolved salts (TDS) (mg/L)		pH		IC method			Proposed method		
Before adsorption	After adsorption	Before adsorption	After adsorption	C ₀ (mg/L)	C _e (mg/L)	R %	C ₀ (mg/L)	C _e (mg/L)	R %
793	781	7.05	6.96	2.134	0.133	94	1.862	0.167	91
A spiked Nile River sample									
Total dissolved salts (TDS) (mg/L)		pH		IC method			Proposed method		
Before adsorption	After adsorption	Before adsorption	After adsorption	C ₀ (mg/L)	C _e (mg/L)	R %	C ₀ (mg/L)	C _e (mg/L)	R %
211	196	7.06	6.92	5.063	0.185	96	5.021	0.284	94
Wastewater after the tertiary treatment process									
Total dissolved salts (TDS) (mg/L)		pH		IC method			Proposed method		
Before adsorption	After adsorption	Before adsorption	After adsorption	C ₀ (mg/L)	C _e (mg/L)	R %	C ₀ (mg/L)	C _e (mg/L)	R %
631	624	7.03	6.89	4.552	0.451	90	4.273	0.474	89

Table 5: Comparison between adsorption capacity of PH, mPH and BPH with other adsorbents toward NH₄ (I).

Adsorbent	q _{max} (mg/g)	Conditions				Ref.
		pH	T (°C)	Dose (g/L)	Contact time (min)	
PH	1.45	7	25	3	100	This work
mPH	2.16	7	25	3	100	This work
BPH	3.08	7	25	3	100	This work
Posidonia oceanic(L) fibers	1.97	6	18	3	40	[34]
Coconut shell derived AC	2.3	9	10	40	120	[35]
Rice husk derived AC	3.24	7	25	20	210	[36]
Paulownia600	2.72	2	----	-	120	[37]
Slag	3.1	9	45	10	150	[38]
S rosthornii Seemen	3.31	7	r.t	4	1440	[39]
Maple wood biochar	0.87	7	r.t	12.5	960	[40]
PS300	5.38	7	20	3	720	[41]
Eupatorium Adenophora biochar	1.91	8	25	12.5	-	[42]
WS550	2.08	7	20	3	1440	[41]
Al-modified Orange Tree	1.77	-	25	10	440	[43]
Sugarcane bagasse ash	0.32	8	40	20	180	[10]
Pine wood chips biochar	3.68	7	25	1	120	[44]
Giant reed straw derived biochar	1.49	8	40	50	25	[45]
Iron@AC	0.46	7	25	-	240	[46]
Lignite	3.43	8	25	20	10	[47]
Natural zeolite	3.11	7	25	-	30	[48]
Pumice	0.28	7	23	100	180	[49]
Bentonite I	4.92	-	r.t	100	180	[50]
Activated natural zeolite	2.94	7	30	10	900	[51]
Modified Chinese medical stone	3.50	6	25	5	120	[52]
Ultrasound-modified zeolite	2.10	7	20	20	45	[53]
Na ⁺ impregnation AC	1.19	6.43	25	5	120	[54]
Barbecue bamboo charcoal	1.75	9	30	4	80	[55]
Giant reed straw	1.49	8	40	50	25	[46]
Fly ash	0.30	7.5	20	20	120	[56]
K ₂ CO ₃ -activated oil palm shell biochar	1.49	-	-	6	1440	[57]
Fe ₃ O ₄ supported sludge biochar	1.78	-	35	20	600	[58]

5. Conclusions

In our study, $\text{NH}_4(\text{I})$ ions remediation from their aqueous solutions by pure PH powder, modified PH (m-PH), and biochar derived from PH (BPH). The results indicate that the adsorption capacity of both m-PH, and BPH derived materials are higher than that of the pure PH, this mainly due to increasing surface area. The adsorption isotherm verifies that the adsorption of $\text{NH}_4(\text{I})$ ions onto the BPH fits the Freundlich model, while the adsorption onto the PH and mPH obeyed Langmuir model. Moreover, the kinetic analysis showed that the experimental data is well fitted by the pseudo-second-order model. For practical applications, our prepared materials showed promising re-usability for five consecutive cycles of adsorption-desorption. Also, the prepared adsorbent materials showed potential applicability toward remediation of ammonium ions from real sample which is significant important for practical uses in large scale. The finding in our study opens the way for future study in preparing PH derived nano materials such as metal oxides dispersed in porous carbon derived from PH, as well as chemical modification of PH powder by various substances with functional groups such as amino-, carbonylated-based materials to be investigate their adsorptive ability toward various pollutants from the aqueous systems.

Conflict of interest:

The authors declare there are no conflicts.

6. References

- Rafaqat, S.; Ali, N.; Torres, C.; Rittmann, B. *RSC Adv.*, *12*, 17104-17137 (2022).
- Chan, M.K.; Yeow, A.T.Z. *IOP Conference Series: Mater. Sci. Eng.*, *1092*, 012073 (2021).
- Dey, S.; Taraka Naga Veerendra, G.; Anjaneya Babu Padavala, S.S.; Phani Manoj, A.V. *Water-Energy Nexus*, *6*, 187-230 (2023).
- Dey, S.; Charan, S. S.; Pallavi, U.; Sreenivasulu, A.; Haripavan, N. *Energy Nexus*, *7*, 100119 (2022).
- Chen, Y.; Jiang, D.-D.; Yang, K.-H.; Zhu, X.; Kong, L.-Y.; Li, X.-W.; Deng, S.-P.; *China Environ. Sci.*, *42*, 3265 (2022).
- Dey, S.; Haripavan, N.; Basha, S.R.; Babu, G.V. *Curr. Res. Chem. Biology*, *1*, 100005 (2021).
- Randall, D.J.; Tsui, T.K.N. *Mar. Poll. Bullet.*, *45*, 17-23 (2002).
- Alijani Galangashi, M.; Masoumi Kojidi, S.F.; Pendashteh, A.; Abbasi Souraki, B.; Mirroshandel, A.A. *J. Water Process Eng.*, *39*, 101714 (2021).
- Wahab, M.A.; Jellali, S.; Jedidi, N. *Bioresour. Technol.*, *101* (2010).
- Mor, S.; Negi, P.; Ravindra, K. *Environ. Sci. Pollut. Res. Int.*, *26*, 24516-24531 (2019).
- Fseha, Y.H.; Sizirici, B.; Yildiz, I. *J. Environ. Chem. Eng.*, *9*, 106598 (2021).
- Hasan, M.N.; Altaf, M.M.; Khan, N.A.; Khan, A.H.; Khan, A.A.; Ahmed, S.; Kumar, P.S.; Naushad, M.; Rajapaksha, A.U.; Iqbal, J.; et al. *Chemosphere*, *277*, 130328 (2021).
- Feng, L.; Qiu, T.; Yan, H.; Liu, C.; Chen, Y.; Zhou, X.; Qiu, S. *Water, Air, Soil Pollut.*, *234*, 280 (2023).
- Yongxiang N.; Chao Z.; Yucong X.; Kai K.; Hua S.; Shupeil B.; Hao H.; Shunyi L. *Nanomaterials*, *13*, 2857 (2023).
- Bowen L.; Yinlong Z.; Wanlin G. *Inorg. Chem. Front.*, *10*, 5812-5838 (2023).
- Wahab, M.A.; Jellali, S.; Jedidi, N. *Bioresour. Technol.*, *101*, 5070-5075 (2010).
- Wang, X.; Lü, S.; Gao, C.; Feng, C.; Xu, X.; Bai, X.; Gao, N.; Yang, J.; Liu, M.; Wu, L. *ACS Sustainable Chem. Eng.*, *4*, 2068-2079 (2016).
- Azreen, I.; Lija, Y.; Zahrim, A.Y. *IOP Conference Series: Mater. Sci. Eng.*, *206*, 012077 (2017).
- Ahmed, A.S.A.; Xiang, W.; Abdelmotalleib, M.; Zhao, X. *ACS Appl. Electron. Mater.*, *4*, 1063-1071 (2022).
- Ramrakhiani, L.; Ghosh, S.; Majumdar, S. *Appl. Biochem. Biotechnol.*, *180*, 41-78 (2016).
- Ricky, L.N.S.; Shahril, Y.; Nurmin, B.; Zahrim, A.Y. *IOP Conference Series: Earth Environ. Sci.*, *36*, 012055 (2016).
- Abdelfattah, I.; El-Saied, F.A.; Almedolab, A.A.; El-Shamy, A. M. *Appl. Biochem. Biotechnol.*, *194*, 4105-4134 (2022).
- Yang, H.; Li, X.; Wang, Y.; Wang, J.; Yang, L.; Ma, Z.; Luo, J.; Cui, X.; Yan, B.; Chen, G. *Processes*, *11* (2023).
- Qiu, M.; Liu, L.; Ling, Q.; Cai, Y.; Yu, S.; Wang, S.; Fu, D.; Hu, B.; Wang, X. *Biochar*, *4*, 19 (2022).
- Liu, L.; Zhang, M. *Int. J. Environ. Sci. Technol.*, *20*, 13783-13798 (2023).
- Lazarova, S.; Tonev, R.; Dimitrova, S.; Dimova, G.; Mihailova, I. *Processes*, *11* (2023).
- Herbert, A.; Kumar, U.; Janardhan, P. *Water Environ. Res.*, *93*, 1032-1043 (2021).
- Dey, S.; Basha, S.R.; Babu, G.V.; Nagendra, T. *Clean. Mater.*, *1*, 100001 (2021).
- Jeppu, G.P.; Clement, T.P. *J. contaminant hydrol.*, *129-130*, 46-53 (2012).
- Ayawei, N.; Ebelegi, A.N.; Wankasi, D. *J. Chem.*, *2017*, 3039817 (2017).
- Simonin, J.-P. *Chem. Eng. J.*, *300*, 254-263 (2016).
- Wang, J.; Guo, X. *Chemosphere*, *309*, 136732 (2022).
- Nessma S. M. S.; Abdelaal S. A. A.; Mohamed H. A.; Gamal A. G.; *Sci Rep* *14*, 5384 (2024).34.

34. Jellali, S.; Wahab, M.A.; Anane, M.; Riahi, K.; Jedidi, N. *Desalination*, 270, 40-49 (2011).
35. Boopathy, R.; Karthikeyan, S.; Mandal, A.B.; Sekaran, G. *Environ. Sci. Pollut. Res. Int.*, 20, 533-542 (2013).
36. Zhu, K.; Fu, H.; Zhang, J.; Lv, X.; Tang, J.; Xu, X. *Biomass Bioenerg.*, 43, 18-25 (2012).
37. Sayadi, M.; Farasati, M.; G. Mahmoodlu, M.; Rostami Charati, F. *Iran. J. Chem. Chem. Eng.*, 39, 205-222 (2020).
38. Zhang, L.Y.; Zhang, H.Y.; Guo, W.; Tian, Y.L. *Inter. J. Environ. Sci. Technol.*, 10, 1309-1318 (2013).
39. Zeng, Z.; Zhang, S.D.; Li, T.Q.; Zhao, F.L.; He, Z.L.; Zhao, H.P.; Yang, X.E.; Wang, H.L.; Zhao, J.; Rafiq, M.T. *J. Zhejiang Univ. Sci. B*, 14, 1152-1161 (2013).
40. Wang, B.; Lehmann, J.; Hanley, K.; Hestrin, R.; Enders, A. *RSC Adv.*, 6, 41907-41913 (2016).
41. Yang, H.I.; Lou, K.; Rajapaksha, A.U.; Ok, Y.S.; Anyia, A.O.; Chang, S.X. *Environ. Sci. Pollut. Res. Int.*, 25, 25638-25647 (2018).
42. Cheng, N.; Wang, B.; Feng, Q.; Zhang, X.; Chen, M. *Bioresour. Technol.*, 340, 125696 (2021).
43. Salimova, A.; Zuo, J.e.; Liu, F.; Wang, Y.; Wang, S.; Verichev, K. *Front. Environ. Sci. Eng.*, 14, 48 (2020).
44. Rezaee, M.; Gitipour, S.; Sarrafzadeh, M.-H. *Environ. Eng. Manage. J.*, 20 (2021).
45. Hou, J.; Huang, L.; Yang, Z.; Zhao, Y.; Deng, C.; Chen, Y.; Li, X. *Environ. Sci. Pollut. Res. Int.*, 23, 19107-19115 (2016).
46. Ren, Z.; Jia, B.; Zhang, G.; Fu, X.; Wang, Z.; Wang, P.; Lv, L. *Chemosphere*, 262, 127895 (2021).
47. Tu, Y.; Feng, P.; Ren, Y.; Cao, Z.; Wang, R.; Xu, Z. *Fuel*, 238, 34-43 (2019).
48. Gupta, V.K.; Sadegh, H.; Yari, M.; Shahryari Ghoshekandi, R.; Maazinejad, B.; Chahardori, M. *Glo. J. Environ. Sci. Manag.*, 1, 149-158 (2015).
49. Masoud, M.; Mehdi, F.; Meghdad, P.; Yadollah, M.; Toubia, K.; Kiomars, S. *Arch. Environ. Protec.*, 42, 33-43 (2016).
50. Seruga, P.; Krzywowska, M.; Pyżanowska, J.; Urbanowska, A.; Pawlak-Kruczek, H.; Niedźwiecki, Ł. *Molecules*, 24 (2019).
51. Safie, N.N.; Zahrim Yaser, A.; Hilal, N. *Asia-Pacific J. Chem. Eng.*, 15, e2448 (2020).
52. Arefe, A.; Song, X.; Wang, Y.; Si, Z.; Abayneh, B. *Res. Chem. Intermed.*, 46, 2035-2054 (2020).
53. Zieliński, M.; Zielińska, M.; Dębowski, M. *Desalination Water Treat.*, 57, 8748-8753 (2016).
54. Shi, M.; Wang, Z.; Zheng, Z. *J. Environ. Sci.*, 25, 1501-1510 (2013).
55. Zhou, Z.; Yuan, J.; Hu, M. *Environ. Prog. Sustain. Energy*, 34, 655-662 (2015).
56. Uğurlu, M.; Karaoğlu, M.H. *Microporous Mesoporous Mater.*, 139, 173-178 (2011).
57. Munar-Florez, D.A.; Varón-Cardenas, D.A.; Ramírez-Contreras, N.E.; García-Núñez, J.A. *Results. Chem.*, 3, 100119 (2021).
58. Zhang, L.-J.; Zhang, X.; Liang, H.-F.; Xie, Y.; Tao, H.-C. *Clean. Technol. Environ. Policy*, 20, 2181-2189 (2018).